FILE COPY
DO NOT
REMOVE

ASHRAE
TRANSACTIONS

SYMPOSIUM PAPERS

PRESENTED AT THE

1986 ANNUAL MEETING

IN PORTLAND, OREGON

OF THE

AMERICAN SOCIETY OF HEATING, REFRIGERATING

AND AIR-CONDITIONING ENGINEERS, INC.

1986

VOLUME 92, PART 2B

PO-86-04 No. 3

REAL-TIME IN-SITU REFRACTOMETER FOR CONCENTRATION MEASUREMENTS IN ABSORPTION MACHINES

D.T. Bostick **L.N. Klatt, Ph.D.**

J.E. Strain **H. Perez-Blanco, Ph.D.**
ASHRAE Member

ABSTRACT

An in-situ, real-time refractometer has been developed for the measurement of absorbent concentration in absorption machines. The refractive index of the absorber fluid is determined by measuring light loss from optical fiber cables that are immersed in the solution. The optical fibers have been modified by removing a portion of the cladding from the center of hard clad fiber optics to expose a segment of the core. The exposed portions of the fiber cores are placed at points within an absorption machine for which the measurement of absorbent concentration is desired. The entrance face of all modified fibers is illuminated with a light source. The amount of light lost from the core of each fiber to the absorber solution surrounding the fiber is measured and is directly related to the refractive index of the solution. Because the refractive index of a solution is a function of temperature, a thermocouple junction is placed adjacent to each of the exposed fibers to measure and compensate for local solution temperature. The composition of the absorber fluid is determined from the refractive index through use of an independently determined equation.

INTRODUCTION

Current efforts in absorption technology have been directed toward developing more efficient heating and cooling systems for building temperature control and for the generation of process heat for industrial applications. New working fluids and/or modifications in machine design are being applied in prototypical advanced cycle absorbers to improve machine efficiency. The operation of such advanced cycle absorbers is considerably more complex than conventional heat pump systems. To realize the efficiency inherent in the advanced cycle systems, the machine's operating parameters must be tightly controlled relative to those required in the operation of conventional equipment.

The measurement of absorbent concentration is a key control parameter in operating and assessing the performance of prototypical advanced cycle machines. To be useful, this measurement must not only be accurate, but should also provide real-time data so that the transient behavior within a system can be followed. The capability of determining the concentration of the absorbent at any point inside the machine is also essential to understand and design the advanced heat exchangers required in the new machines.

An analytical tool with the above characteristics would not only be useful for the assessment of prototypical advanced cycle systems but would find wide utility in the control of conventional absorption equipment. To encompass the analytical needs of both types of absorber equipment, a generic concentration monitor would need to operate in a variety of refrigerant/absorbent fluids over a wide range of temperatures and pressures. Subatmospheric to 400 psia (27.5 kPa) pressures and temperatures of a few degrees up to 300°C are typically encountered. Absorbent concentration in conventional absorber machines ranges from 40% to 65% salt by weight in the lithium bromide/water systems and 5% to 60% in the ammonia/water systems. Binary

D. T. Bostick, L. N. Klatt, and J. E. Strain are analytical chemists, Analytical Chemistry Division, Oak Ridge National Laboratory, Oak Ridge, TN 37831; H. Perez-Blanco is a mechanical engineer, Energy Division, Oak Ridge National Laboratory, Oak Ridge, TN 37831.

organic refrigerant/absorbent mixtures incorporated in some prototypical systems are present at comparable levels of concentration. Absorbents in ternary mixtures under consideration, such as lithium bromide/water/ammonia, also fall within the same concentration range.

To date, no analytical technique exists for the real-time measurement of absorbent concentration. Typically, samples are withdrawn from the machine, usually from a single location, and are analyzed by laboratory methods appropriate for the analyte. This discrete sampling method prevents real-time measurement and introduces uncertainties related to obtaining a representative sample.

Because the measurement of absorbent concentration is required in a number of different chemical systems, an analytical technique that is based on the measurement of a general solution property of a binary mixture would most easily be applied to any measurement need in absorber technology. Of the number of properties available, solution refractive index could readily provide in-situ, real-time concentration measurement in binary mixtures. Such a measurement scheme has recently been applied to the analysis of oils (Takeo and Hattori 1982) and salinity in thermohaline solutions (Bergman et al. 1985). The sensing unit in the refractive index monitor is a bent optical fiber in which part of the cladding has been removed. If the bend radius remains constant, the light emerging from the curved fiber is dependent upon the refractive index of the solution surrounding the fiber. With the appropriate selection of bend radius and length of fiber optic core exposure, the measurement of the refractive index is accurate to three decimal places. A thermocouple junction is attached to the refractive index probe to provide a correction for the solution temperature.

The refractive index probe could provide real-time measurement of transient concentration changes of the absorbent in conventional and prototypical absorber equipment. The major difficulty in applying the probe to heat pump equipment would be the ability to install and maintain the geometry of the curved optical fiber along the heat exchange tubes of the absorber machines. Previous applications (Bergman et al. 1985) described shifts in detector response that were attributed to slight changes in the fiber's bend radius. This report describes the use of a stripped optical fiber to monitor the refractive index and, hence, the weight percent concentration of lithium bromide/water solutions. The geometry of the current refractive index probe is altered; the stripped fiber optic is not bent but operates in a straight line defined by the heat exchange tubes. Such a design simplifies the installation of the refractive index monitor within the absorber equipment and also alleviates measuring inaccuracies arising from changes in fiber geometry. This report presents the theory of operation of such a monitor and provides data from a miniabsorber equipped with two fiber optics mounted within the vessel.

SINGLE OPTICAL FIBER SYSTEM

Experimental Design

A single optical fiber model of the heat pump refractometer, shown schematically in Figure 1, was assembled to determine the response for LiBr as the heat exchange fluid. All components of the model were secured on an optical rail. Custom mounts were fabricated to rigidly terminate the measurement optical fiber to the tungsten filament light source and the silicon diode detector. A second optical fiber and detector served as a reference signal to correct for light source instability. The voltage from both detectors was amplified and measured with a digital multimeter.

Hard clad silica (HCS) optical fibers were used in these experiments. The cladding of most other fibers is a plastic sleeve surrounding the core. The advantage of HCS fibers over other optical fibers is that the polymeric cladding is chemically bonded to the fused silica core. In the current application, a bonded cladding alleviates the problem of solution seeping between the core and cladding after a portion of the cladding is removed to expose the quartz core.

Cladding was stripped from the center of one-meter lengths of fiber by scoring both the circumference and length of the cladding to be removed with a heated metal rod. The severed cladding was then peeled away from the quartz core; an organic solvent was used to clean the stripped 0.4-1.6 in (10-40 mm) core surface. The ends of the fibers were scored with a sapphire crystal prior to cleavage, forming flat surfaces that were butted against the source and detector faces. The prepared optical fiber was jacketed with a glass flow cell equipped with a calibrated thermistor. Compression connectors and graphite ferrules were used to seal the fiber optics within the flow cell.

Test Procedures

LiBr solutions of known refractive index were pumped through the flow cell from a heated, stirred reservoir. These solutions were prepared on a weight/weight percent basis from 99%+ purity anhydrous LiBr. The standards were analyzed using flame emission to determine the lithium concentration.

Using a refractometer, the relationship between refractive index at 25°C and weight/weight percent LiBr was found to be:

$$n_D^{25°C} = 0.0000241*[LiBr]^2 + 0.00108*[LiBr] + 1.3348. \quad (1)$$

The refractive index of LiBr solutions decreases linearly with increasing temperature. The temperature dependence is -0.000106 refractive index unit per °C; this value is independent of LiBr concentration over the range of 0% to 60% (w/w) LiBr.

Theoretical Considerations

The theoretical response of the optical fiber refractometer can be approximated using meridional ray analysis. Referring to Figure 2, in which a light ray is incident on the face of an optical fiber, the angle of the refracted ray can be calculated from Snell's Law (Kapany 1967):

$$n_{air} * \sin(\Theta_I) = n_{fiber} * \sin(\Theta_R) \quad (2)$$

where n is the refractive index, Θ_I is the incident angle, and Θ_R is the refracted angle, both with respect to the fiber axis. The refractive indexes of air and fused quartz are 1.00 and 1.46, respectively. The refracted ray travels through the silica core until it strikes the core-cladding interface at the complementary angle of $90°-\Theta_R$, or Θ_B. Θ_B must be greater than the critical angle, Θ_C, of this interface, defined as

$$\Theta_C = \mathrm{Arcsin}(n_{cladding}/n_{core}), \quad (3)$$

for the ray to be totally internally reflected. The refractive index of the cladding of typical fibers with quartz cores is approximately 1.41, which results in the maximum acceptance angle of an incident ray being approximately 23°. The internally reflected ray will then be repeatedly reflected at the core-cladding interface until the ray emerges from the other end of the fiber or until the ray encounters an interface with a different refractive index.

This latter condition arises where the cladding has been removed from a portion of the fiber and the core is surrounded by LiBr solution. The angle at which the light ray is refracted from this interface (Θ_S) becomes a function of LiBr concentration, as defined in Equation 4.

$$\sin(\Theta_S) = \sin(\Theta_B) * 1.46/n_{LiBr} \quad (4)$$

Figure 2 illustrates the path of an incident ray at various LiBr concentrations. As LiBr concentration increases, the light ray is increasingly bent into the surrounding solution and an increasing fraction of the original ray intensity is lost. Under these conditions a fraction of the light is also reflected back into the fiber at the core-solution interface. The intensity of the reflected ray can be calculated from Fresnel's reflectance equation (Strobel 1973):

$$\text{Reflectance} = \frac{1}{2} \cdot \left[\frac{\sin^2(\Theta_B-\Theta_S) + \tan^2(\Theta_B-\Theta_S)}{\sin^2(\Theta_B+\Theta_S) + \tan^2(\Theta_B+\Theta_S)} \right] \quad (5)$$

It follows from the above discussion that the total amount of light observed by the detector depends upon the angle of the incident ray and upon the LiBr concentration. Using Equation 5, the relationship between the reflected light intensity and the refractive index of LiBr solutions for various incident angles can be calculated; these results are summarized in Figure 3. The relationship is approximately sigmoidal and indicates that, as the incident angle increases, the concentration at which light is no longer totally internally reflected from the core-solution interface shifts to lower LiBr concentrations. The operating range for LiBr analysis can therefore be adjusted to some extent by appropriate selection of the incident angle.

Results

A multivariant experiment was conducted on the single fiber instrument to determine and compare the optimum optical fiber diameter, fiber exposure length, and observed LiBr concentration profile with the predicted theoretical response. The observed optical response from the single fiber instrument, in which 0.5 in (13 mm) of cladding was removed, is illustrated in Figure 4. The voltage response, normalized with respect to the reference fiber signal, presents a concentration profile similar to that developed through theoretical considerations. The incident angle is not discrete in this instrument but includes all angles from 0 to 23°.

In Figure 4 the refractive index profiles for a LiBr solution at three different temperatures are shown. As the temperature increases from 30 to 45°C, the observed light levels increase for a given concentration of LiBr. This temperature effect is inherent in Equation 5, because the refractive index of LiBr solutions decreases by ∿ 0.0001 refractive index units per °C increase in solution temperature.

Because meridional ray analysis of an optical fiber is only an approximation, the equations presented in the theory section cannot be used to directly calculate the LiBr concentration from the observed transmitted light levels and solution temperatures. Instead, an empirical relationship, as a function of temperature and concentration, was developed from the observed instrumental data. Figure 5 shows the relationship between the observed voltage, V_{obs}, and temperature for five LiBr solutions of known refractive index. The relationship for each LiBr solution is described by a first-order polynominal in temperature:

$$V_{obs} = V^{o}_{n_D} + E_{n_D} * T \tag{6}$$

Both $V^{o}_{n_D}$ and E_{n_D} are dependent upon the concentration of the sample, as shown in Figures 6 and 7. Over the refractive index range of 1.43-1.47 these two parameters can be described by:

$$V^{o}_{n_D} = A * n_D^2 + B * n_D + C \tag{7}$$

and

$$E_{n_D} = F * n_D^2 + G * n_D + H \tag{8}$$

Equations 6-8 can be combined to yield an expression for the observed voltage at a given LiBr solution as a function of temperature and its refractive index:

$$V_{obs} = (A + FT) * n_D^2 + (B + GT) * n_D + (C + HT) \tag{9}$$

The numerical values of coefficients A through G are established with LiBr standards of known refractive index. The refractive index of unknown LiBr solutions is determined by measuring the observed voltage and experimental temperature and solving Equation 9 for the corresponding root. The weight/weight percent concentration of LiBr at 25°C in unknown solutions is then calculated from Equation 1.

MINIABSORBER SYSTEM

Experimental Design

The fiber optic refractometer was installed within a miniabsorber to demontrate its utility in determining the real-time concentration of lithium bromide along the heat exchange tubes. A block diagram of the system used for the absorption experiments is shown in Figure 8. The major components include a miniabsorber, an optical system, and a computer-controlled data acquisition system.

The miniabsorber was constructed from a six-inch-diameter, 7/32-inch wall, section of 304L stainless steel pipe. Hemispherical end-caps were welded to the ends of the pipe to close the system. The water coolant was circulated through two U-shaped tubes, 3/8 inch o.d., which penetrated one of the end-caps. A viewing window was attached to the top of the vessel to allow access to the inside, as well as allowing one to observe the droplet formation during the operation of the system. The miniabsorber was designed to withstand pressures and temperatures up to 300 psia (20.6 kPa) and 500 F (260°C), respectively, so that both lithium bromide/water and ammonia/water absorption experiments could be run. The heat exchange fluid was recirculated by a small centrifugal pump. Thermocouples and optical fibers were installed in the test vessel with glands. A port in the vessel was provided to allow attachment of a vacuum pump for operation at reduced pressures. The heat exchange fluid in the sump of the test vessel was heated by a strap heater attached to the underside of the vessel. A heating tape was wrapped around the pipe carrying the heat exchange fluid from the pump back to the test vessel. Pump speed and heater power were controlled manually through the use of autotransformers.

Thermocouples (stainless steel sheathed, chromel-alumel) were used to monitor the temperature of the liquid film on the heat exchange tubes; these were attached to the heat exchange tubes with short lengths of wire. Additional thermocouples were used to measure the temperature of the recirculating fluid at the exit port of the test vessel and to measure the temperature of the coolant at the entrance and the exit of each heat exchange tube.

The optical fibers were attached to the lower surface of the heat exchange tubes with stainless steel clips. Light from a tungsten filament lamp was multiplexed through the measurement and reference fibers with the aid of a multiplexer wheel rotated by a 6 rpm synchronous motor. Because of the apertures resulting from this source multiplexer arrangement, only about 3 degrees of the optical fiber acceptance cone was illuminated. Timing signals for the data acquisition system were generated from light pulses produced by an outer set of holes in the multiplexer wheel.

A single silicon photodiode served as the optical detector. The output current from the photodiode was converted to a voltage through use of the current-to-voltage converter circuit.

The thermocouple voltages and output of the optical detector were digitized with a digital voltmeter used in conjunction with a data acquisition/control unit. These modules were controlled with a minicomputer; data were stored on magnetic tape.

Test Procedures

The test vessel was originally equipped with four 1000 μ diameter optical fibers. Because these fibers are easily broken after the cladding is removed, a support of sufficient length to bridge the stripped area was fabricated by cutting away the upper portion of thin wall stainless steel tubing, drilling holes in the lower portion, and attaching it to the optical fiber with epoxy adhesive. After numerous unsuccessful attempts to calibrate the system, these fibers were removed from the test vessel; upon examination it was found that foreign material had deposited on the stripped optical fiber and had collected between the fiber and the support. Two 600 μ diameter fibers were then installed in the test vessel on heat exchange tubes number one and two. Because these smaller fibers are less susceptible to breakage, a support system was not required. All absorption data reported herein were acquired with this two-fiber arrangement.

The heat absorption experiments were performed as follows. Approximately 650 mL of 55 (w/w)% LiBr solution was added to the test vessel and the unit sealed. A vacuum pump was attached to the system and the vessel pumped down to approximately 29 inches of mercury (3 kPa); the pumping rate was then adjusted to maintain approximately this pressure. Electrical

power was supplied to the heaters; the fluid circulating pump and the water coolant flow were started. When the temperature of the LiBr solution exiting from the sump of the test vessel reached approximately 65°C, data acquistion was initiated. Data for each run were collected for periods of four minutes at twenty-second intervals. Although the flow rate of the recirculating LiBr solution was nominally adjusted to yield rapid but discrete droplet formation on the drip tube, it was extremely difficult to maintain this flow condition. The actual delivery of the LiBr to the heat exchange tubes pulsed as though vapor was forming in the recirculating lines.

Calibration data were acquired immediately after completion of the absorption experiment. The system was cooled to approximately 30°C and the test vessel opened. The flow rate of the recirculating LiBr was increased to produce a steady stream from the drip tube. Samples of the LiBr solution were withdrawn and the refractive index recorded with a refractometer. The signals from the two optical fibers and the corresponding temperatures were recorded. Distilled water was added to the test vessel, the solution allowed to mix, and the next set of refractive index, optical, and temperature data were recorded. These steps were repeated until the LiBr solution was diluted to approximately 45 (w/w)%.

Results

The principal noise component of the optical signals was a 120 Hz signal resulting from operation of the lamp with 60 Hz power. This component was removed by programming the digital voltmeter to synchronously integrate the input signal for 10 power line cycles. Integration was initiated 0.05 seconds after receipt of the trigger signal to ensure that the measurement was performed on the plateau of each optical signal. The typical dark current under these conditions was 340±6 μV; the optical voltage from the reference and two measurement fibers was between 2 and 8 volts with a standard deviation of 2-6 mV.

The long-term stability of the source and detector was determined by recording the normalized signals (signals from the sample fibers divided by the signal from the reference fiber) for one-hour intervals at random times during a span of three days. The source power was turned on at the beginning and off at the end of each day. A typical set of data for a one-hour interval is shown in Figure 9. The stability of the optical signal for two fibers averaged over the three-day period was 0.9245±0.0039 and 0.9106±0.0026. The results from both the short- and long-term stability studies indicate an average short-term stability < 0.2% and an average long-term stability < 0.5%.

Experiments were conducted that verified that, except for the signal change resulting from the temperature dependence of the refractive index of the LiBr solutions, the optical signals are independent of temperature.

Four successive data sets acquired during a heat absorption experiment are presented in Table 1. The experimental data were obtained using water as the coolant circulating at a rate of one gallon per minute. The inlet temperature was 17.2°C; the outlet temperature was 18.3°C. The strap heater and heating tape power were maintained at 400 and 130 watts, respectively; the latter heat input approximately balanced the heat lost in the recirculating lines. The total elapsed time from initiation of data acquisition for set number one to the completion of set number four was 34 minutes. The test vessel was at operating temperature and pressure for approximately two hours before these data were acquired. The flow rate of the recirculating LiBr solution required adjustment just prior to acquisition of the fourth data set.

Calibration data obtained immediately after termination of the absorption experiment are summarized in Table 2.

DISCUSSION

Single Optical Fiber System

The accuracy and utility of the fiber optic refractometer was established in the single optical fiber system and with the multi-fiber absorption test system. Table 3 summarizes the numerical values of the coefficients in Equation 9 for the 1000 μ fiber with a 0.5 in (13 mm) core length exposure. Also tabulated is the correspondence between the known refractive index of LiBr solutions at 25°C and those predicted using the observed voltage and measured temperature. The standard deviation between the known and predicted LiBr concentration is 0.3%.

Similar LiBr concentration profiles and temperature studies were repeated using 600 and 400 μ fibers. The total amount of light transmitted through the fiber decreased by a factor of 4 and 10 for the 600 and 400 μ fibers, respectively. The optical response for both fiber diameters exhibited the same second-order dependence on solution concentration and temperature as that observed with the 1000 μ diameter fiber. Although the 1000 μ fiber had a slightly greater signal-to-noise ratio than either of the other fibers, it is mechanically so rigid that it is easily broken during cladding removal. The 600 μ fiber is sufficiently flexible that breakage is rare, while the 400 μ fiber was too easily broken to be useful.

The effect of the length of core exposure on observed optical response was defined for 1000 and 600 μ fibers. The change in the relative voltage with LiBr concentration is similar to Figure 4 for all exposure lengths greater than 5 mm. The measurement range for LiBr shifts to slightly lower concentrations and the voltage response range increases with increasing fiber exposure length. The optimum exposure length appears to be between 0.5-1 in (10-20 mm), which provides the greatest measurement sensitivity with an adequate signal-to-noise ratio at approximately 60% LiBr.

Miniabsorber System

Figure 10 summarizes the concentration of LiBr measured on the two heat exchange tubes during the absorption experiment. The difference between the mean LiBr concentrations on the two heat exchange tubes for data sets 1-3 are statistically significant at the 95% confidence level. If one uses the last eight and the last four points from heat exchange tubes one and two, respectively, of data set 4, this difference is also statistically significant at the 95% confidence level.

Transferring the concentration data of Figure 10 and the corresponding temperature data of Table V to the equilibrium phase diagram (ASHRAE 1981) for the LiBr-H_2O solutions reveals some inconsistencies in the data. The average values of data sets 1-3 and the average of the last four points of data set 4 are shown in Figure 11. The apparent saturation vapor pressure of the solution on heat exchange tube number one is significantly lower than that on heat exchange tube number two in all cases. On heat exchange tube number two, the equilibrium refrigerant temperatures for data sets 1-2 and 3-4 are not equal. Also, the apparent saturation vapor pressures of the solution on heat exchange tube number two for data sets 1-2 and 3-4 appear to be different. However, within the resolution of the dial pressure gauge attached to the test vessel, this difference may not be significant.

One explanation for these inconsistencies could be that the thermocouple attached to heat exchange tube number one was not measuring the correct temperature. However, this supposition cannot be supported because, during acquisition of the calibration data, the observed temperatures on heat exchange tubes one and two typically differed by <0.1°C over the temperature range of 23-37°C. The possibility that the thermocouple sensed the wall temperature of the heat exchange tube instead of the liquid film cannot be totally excluded.

Two facts support the existence of nonequilibrium conditions. The pulse flow of the LiBr solution from the drip tube, probably caused by formation of vapor within the fluid lines, suggests that the LiBr solution emerging from the drip tube and falling onto heat exchange tube number one is not in thermal and/or mass equilibrium. Second, the significant difference in the recovery of the concentration of LiBr to the steady-state value on heat exchange tube number two relative to that of tube number one also suggests that equilibrium heat and/or mass transfer conditions did not exist.

CONCLUSION

This report demonstrates the utility of a refractive index monitor to determine in real time the concentration of lithium bromide along the heat exchange tubes of an absorber vessel. The straight alignment of the optical fiber, coupled with precise temperature measurement, yielded an analytical measurement accuracy within 0.5 (w/w)% LiBr. Use of multiple optical fibers in the absorber equipment can provide a complete description of LiBr concentration transients at any point within the machine. Because the measurement is based on a general property of binary solutions, the monitor can be applied to other refrigerant/absorbent mixtures having refractive indexes within the 1.4-1.5 range.

REFERENCES

ASHRAE. 1981. ASHRAE handbook--1981 fundamentals. Atlanta: American Society of Heating, Refrigerating, and Air-Conditioning Engineers, Inc., p. 17.142.

Bergman, T. L.; Incropera, F. P.; and Stevenson 1985. "Miniature fiber-optic refractometer for measurement of salinity in double-diffusive thermohaline systems". Rev. Sci. Instrum. Vol. 56, No. 2, pp. 291-296.

Kapany, N. S. 1967. Fiber optics: Principles and applications. New York: Academic Press, Chapter 2.

Strobel, H. A. 1973. Chemical instrumentation: A systematic approach. Reading, MA: Addison-Weseley Publishing Co., Chapter 10.

Takeo, T., and Hattori, H. 1982. "Optical fiber sensor for measuring refractive index." Jpn. J. Appl. Phys. Vol. 21, No. 10, pp. 1509-1512.

ACKNOWLEDGMENT

Research sponsored by the Office of Building and Community Systems, U. S. Department of Energy, under contract DE-AC05-84OR21400 with Martin Marietta Energy Systems, Inc.

TABLE I

Heat Absorption Data

	Data set 1		Data set 2		Data set 3		Data set 4	
Fiber No.	Signal	T°C	Signal	T°C	Signal	T°C	Signal	T°C
1	0.9526	37.1	0.9534	34.1	0.9481	36.0	0.9633	42.2
2	0.5368	42.4	0.5357	44.6	0.5434	46.5	0.5657	44.1
1	0.9498	35.7	0.9516	35.7	0.9469	40.6	0.9577	35.9
2	0.5368	41.3	0.5356	44.8	0.5407	46.4	0.5713	45.0
1	0.9515	34.7	0.9486	34.9	0.9447	40.1	0.9545	39.6
2	0.5388	42.3	0.5349	42.3	0.5415	45.7	0.5712	45.4
1	0.9514	33.1	0.9499	36.1	0.9441	39.6	0.9483	39.7
2	0.5366	42.3	0.5350	43.6	0.5390	47.8	0.5643	45.3
1	0.9513	33.8	0.9495	39.0	0.9441	32.8	0.9461	41.2
2	0.5384	42.7	0.5374	44.1	0.5426	48.1	0.5522	46.3
1	0.9522	32.6	0.9481	40.2	0.9439	35.4	0.9450	36.8
2	0.5372	43.1	0.5348	44.5	0.5397	45.0	0.5498	47.8
1	0.9545	32.3	0.9480	39.5	0.9460	34.2	0.9429	41.3
2	0.5413	42.2	0.5346	31.6	0.5424	45.4	0.5466	39.2
1	0.9506	31.4	0.9495	37.7	0.9451	33.9	0.9473	33.4
2	0.5338	42.6	0.5335	42.0	0.5400	45.5	0.5449	44.6
1	0.9488	35.4	0.9496	38.5	0.9467	34.5	0.9456	33.4
2	0.5385	39.2	0.5323	42.4	0.5388	43.5	0.5440	44.5
1	0.9518	38.5	0.9518	36.7	0.9459	34.9	0.9452	36.2
2	0.5347	33.9	0.5345	44.3	0.5416	45.7	0.5434	45.6
1	0.9528	38.2	0.9538	39.0	0.9441	35.9	0.9447	38.2
2	0.5391	40.0	0.5366	35.6	0.5424	45.2	0.5412	46.0
1	0.9517	37.6	0.9522	35.3	0.9454	34.7	0.9452	34.5
2	0.5373	42.8	0.5350	43.1	0.5425	46.6	0.5413	46.8

TABLE 2

Calibration data

Refractive Index T = 25°C	Solution Temperature, °C	Signal[a] Fiber No. 1	Signal[b] Fiber No. 2
1.4663	34.1	0.9461	0.5337
1.4619	37.3	0.9547	0.5352
1.4579	24.0	0.9597	0.5327
1.4541	29.7	0.9694	0.5369
1.4485	31.1	0.9764	0.5417
1.4405	31.7	0.9822	0.5509
1.4333	31.8	0.9862	0.5596
1.4271	31.5	0.9888	0.5671

[a]mean standard deviation of signal is 0.0011
[b]mean standard deviation of signal is 0.0006

TABLE 3

Comparison of Observed Versus Predicted Refractive Index

Numerical values for coefficents of Equation 9:

A = -294.805 F = 4.3013
B = 846.304 G = -12.3828
C = -606.922 H = 8.9122

[a]Observed n_D	T,°C	V_{obs}	[b]Predicted n_D
1.4667	30.4	0.262	1.4673 (55.0%)
(54.9%)	33.0	0.275	1.4669 (54.9%)
	37.9	0.291	1.4670 (54.9%)
	45.1	0.313	1.4674 (55.1%)
1.4577	29.8	0.3563	1.4577 (52.4%)
(52.4%)	33.0	0.3629	1.4575 (52.4%)
	37.9	0.3700	1.4576 (52.4%)
	45.1	0.3709	1.4594 (52.9%)
1.4525	30.4	0.3969	1.4524 (50.9%)
(51.0%)	33.0	0.4001	1.4523 (51.0%)
	37.9	0.4070	1.4519 (50.8%)
	45.9	0.4094	1.4527 (51.0%)
1.4437	30.0	0.4330	1.4456 (49.0%)
(48.4%)	33.0	0.4354	1.4457 (49.0%)
	37.9	0.4370	1.4457 (49.0%)
	45.1	0.4400	1.4456 (49.0%)
1.4319	33.0	0.4642	1.4347 (45.7%)
(44.9%)	37.9	0.4674	1.4327 (45.1%)
	45.1	0.4683	1.4343 (45.6%)

[a]Value in parentheses is the actual LiBr (w/w)% concentration.
[b]Value in parentheses is the predicted LiBr (w/w)% concentration.

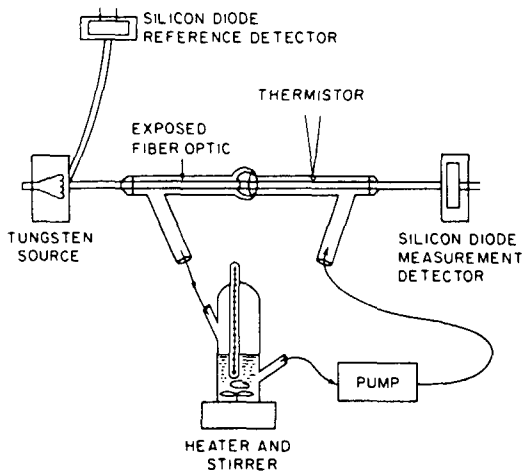

Figure 1. Schematic of single-fiber refractometer

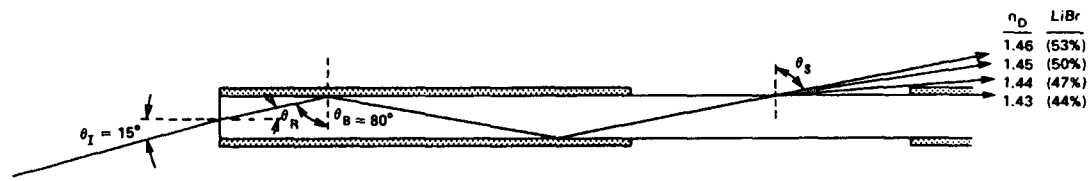

Figure 2. Ray tracing within the fiber optic refractometer

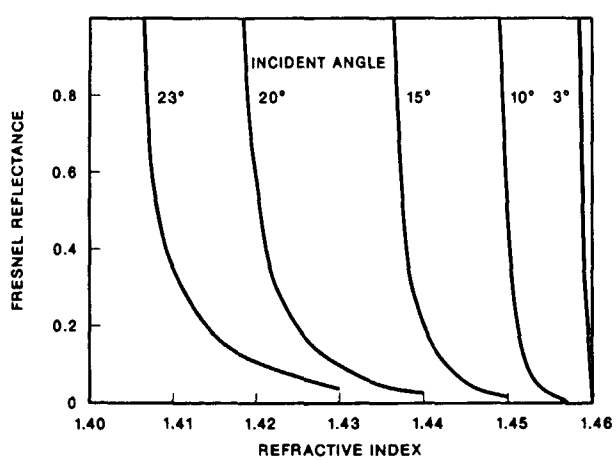

Figure 3. Theoretical reflectance profile as a function of incident light angle

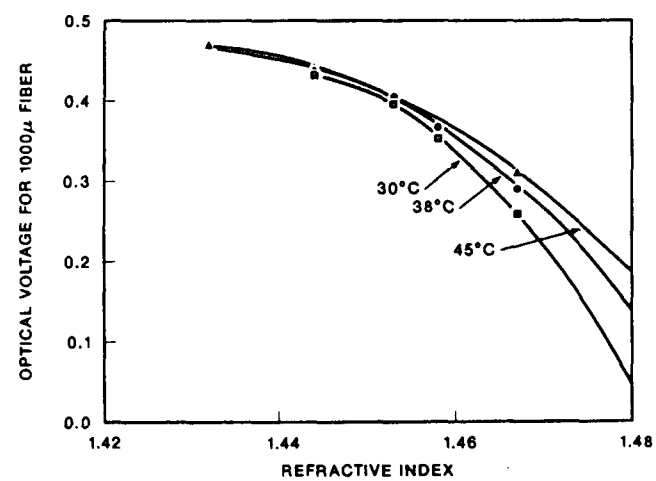

Figure 4. Refractive index profile for a 1000 μ diameter fiber with a 13 mm core exposure length

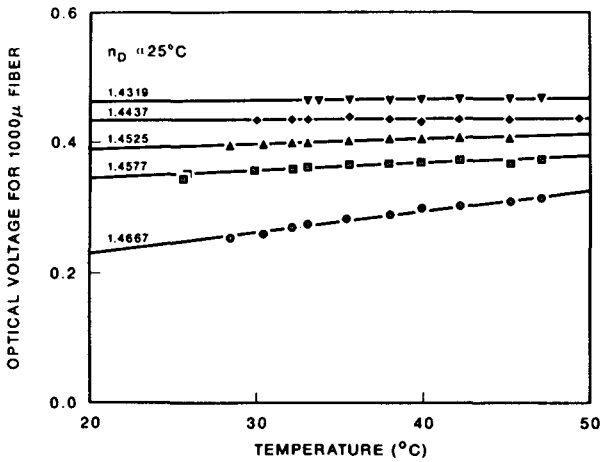

Figure 5. Temperature profile for five LiBr solutions

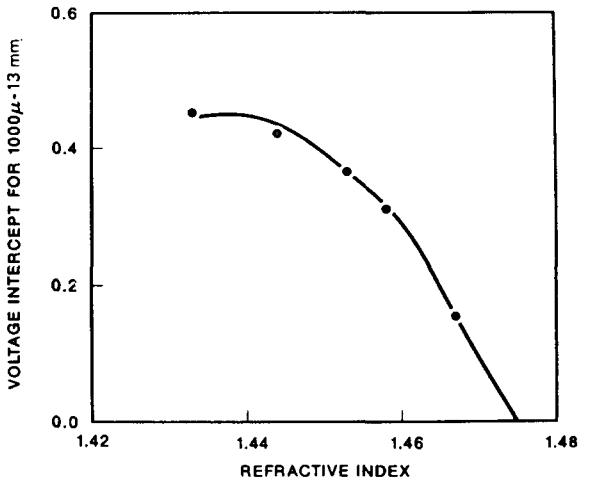

Figure 6. Optical voltage intercept (V°) as a function of refractive index

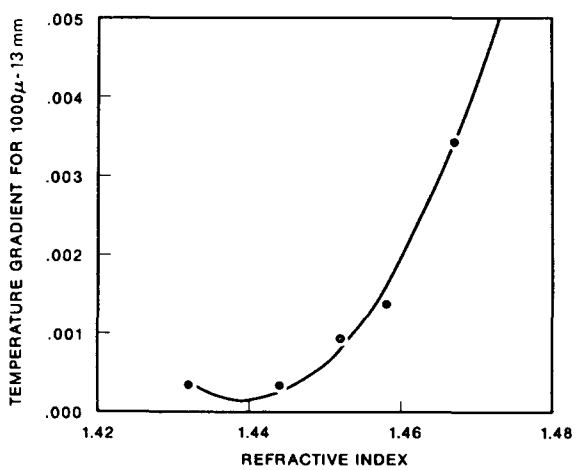

Figure 7. Temperature gradient (E) as a function of refractive index

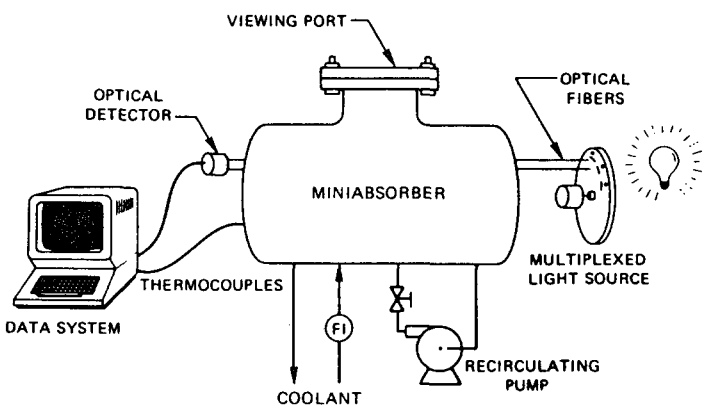

Figure 8. Schematic of the absorption test apparatus

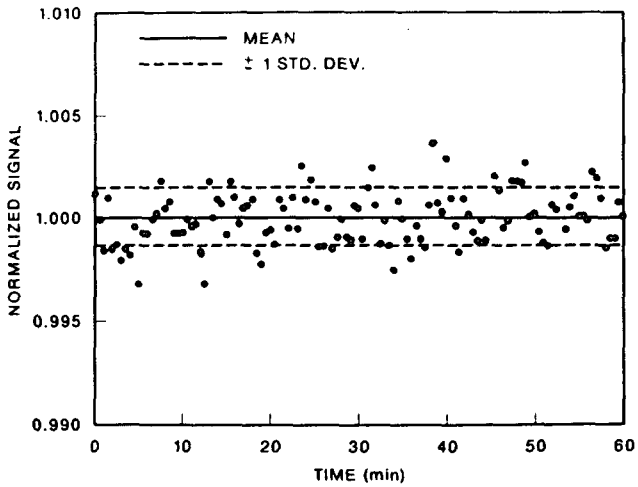

Figure 9. Stability of typical optical signal

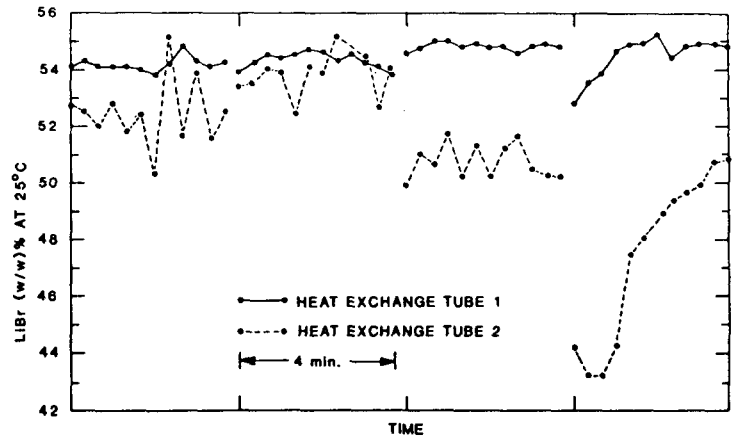

Figure 10. Concentration of LiBr during an absorption experiment

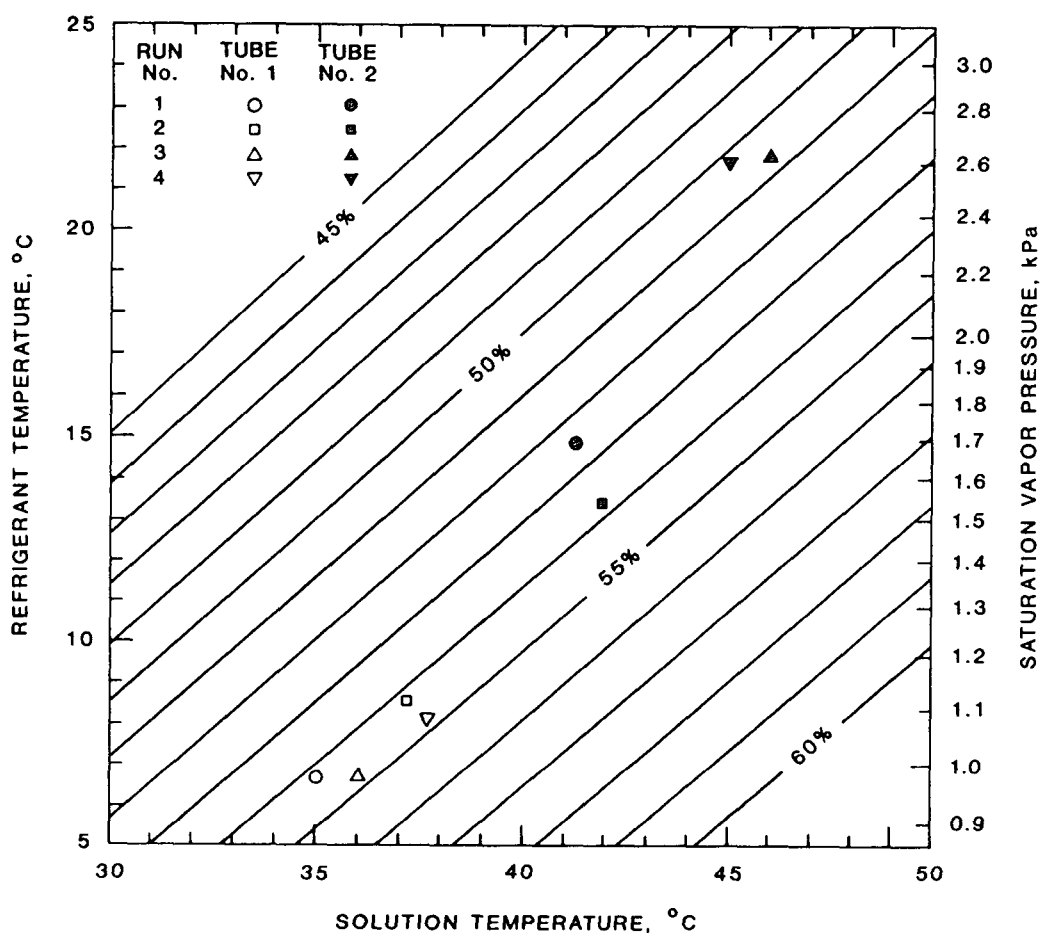

Figure 11. Equilibrium phase diagram for absorption run

Discussion

ROBERT, Inst. of Gas Technology, Chicago: Are there any maximum temperatures beyond which the material of the fiber is affected? Do solution impurities (corrosion inhibitors) affect the measurement?

D. BOSTICK: The operating temperature range of the fibers that are currently used in the instrument is -60° to 125° C. Metal corrosion products from the interior of absorption machines, contaminants in commercial-grade absorbents and refrigerants, and corrosion inhibitors added to absorption fluids represent the three main souces of solution impurities. The impuritites from these sources will not contribute significantly to the total refractive index of the absorption fluid if the concentration of these impurities does not exceed 0.5% by weight and if they do not officially absorb light at the operating wavelength of the light source. If an impurity does absorb light significantly at a given wavelength, a light source is selected for the measurement system that does not emit at this wavelength.

W.T. HANNA, Battelle, Columbus, OH:

1. When for NH_3 cell?
2. Effect of grade of LiBv?
3. Effects of corrosion products/inhibitor?

BOSTICK: Efforts are now underway to modify the current monitoring system for the measurement of ammonia in ammonia/water absorption machines. Questions 2 and 3 are answered above.